PCP
PLANT & CELL PHYSIOLOGY

Far-Red Light Accelerates Photosynthesis in the Low-Light Phases of Fluctuating Light

Masaru Kono[1,*], Hikaru Kawaguchi[2], Naoki Mizusawa[3,4], Wataru Yamori[1], Yoshihiro Suzuki[2] and Ichiro Terashima[1]

[1]Department of Biological Sciences, School of Science, The University of Tokyo, 7-3-1 Hongo, Bunkyo-ku, Tokyo, 113-0033 Japan
[2]Faculty of Science, Kanagawa University, 2946 Tsuchiya, Hiratsuka, Kanagawa, 259-1293 Japan
[3]Department of Frontier Bioscience, Hosei University, Koganei, Tokyo, 184-8584 Japan
[4]Research Center for Micro-Nano Technology, Hosei University, Koganei, Tokyo, 184-0003 Japan
*Corresponding author: E-mail, konom07@bs.s.u-tokyo.ac.jp; Fax, +81-3-5841-4465.
(Received September 26, 2018; Accepted September 26, 2019)

Regular Paper

It is well known that far-red light (FR; >700 nm) drives PSI photochemistry, but its effect on photosynthetic performance has received little attention. In this study, the effects of the addition of FR to red fluctuating light (FL) have on photosynthesis were examined in the leaves of *Arabidopsis thaliana*. Light-activated leaves were illuminated with FL [alternating high light/low light (HL/LL) at 800/30 μmol m^{-2} s^{-1}] for 10–15 min without or with FR at intensities that reflected natural conditions. The CO_2 assimilation rates upon the transition from HL to LL were significantly greater with FR than without FR. The enhancement of photosynthesis by FR was small under the steady-state conditions and in the HL phases of FL. Proton conductivity through the thylakoid membrane (gH^+) in the LL phases of FL, estimated from the dark relaxation kinetics of the electrochromic absorbance shift, was greater with FR than without FR. The relaxation of non-photochemical quenching (NPQ) in the PSII antenna system and the increase in PSII photochemistry in the LL phases accelerated in the presence of FR. Similar FR-effects in FL were confirmed in typical sun and shade plants. On the basis of these results, we concluded that FR exerted beneficial effects on photosynthesis in FL by exciting PSI and accelerating NPQ relaxation and PSII-yield increase. This was probably because of the increased gH^+, which would reflect faster ΔpH dissipation and ATP synthesis.

Keywords: Acceptor-side limitation of PSI • Far-red light • Fluctuating light • Membrane potential • Non-photochemical quenching • Proton motive force.

Editor-in-Chief's Choice

Introduction

Sunlight contains far-red light (FR; 700–800 nm) as well as visible light (400–700 nm). In an open site, the irradiance or photon flux density (PFD) per unit wavelength of FR is comparable to that of the visible light (Gates 1980). As green leaves absorb considerably more visible light than FR (Tasker and Smith 1977, Smith 1982), irradiance per unit wavelength of FR is much greater than that of visible light in a canopy shade. The irradiance also changes dynamically with time in the field. Even in an open site, it changes depending on the elevation of the sun and the cover and movements of clouds. In a canopy, irradiance fluctuates more frequently because of the movement of the leaves and stems.

Plants use visible light or photosynthetically active radiation (PAR) ranging from 400 to 700 nm to drive the linear electron flow (LEF) from water to $NADP^+$, to produce NADPH. When applied solely, FR cannot drive photosynthetic O_2 evolution or CO_2 assimilation (Emerson and Lewis 1943, Emerson et al. 1957, Brody and Emerson 1959). This is known as the 'red drop' effect. However, FR absorbed by PSI pigments oxidizes P700 and drives the cyclic electron flow around PSI (CEF-PSI) (Joliot and Joliot 2005, Joliot and Joliot 2006, Laisk et al. 2010). Both the linear and CEFs are coupled with proton translocation from the stroma to the thylakoid lumen, generating the trans-membrane electrochemical potential difference of protons, or the proton motive force (*pmf*). The *pmf*, which comprised the membrane potential (ΔΨ) and pH difference (ΔpH) (Kramer and Sacksteder 1998, Cruz et al. 2001), is used for adenosine triphosphate (ATP) production by H^+-ATPase.

Under high-light (HL) conditions, the lumenal pH is lowered, which triggers the shift of the PSII antenna system from the light absorption to the heat dissipation mode. The degree of this shift can be assessed as the non-photochemical quenching (NPQ) of chlorophyll (Chl) fluorescence (Yamamoto et al. 1962, Adams et al. 1990). The ΔpH-dependent NPQ is referred to as energy-dependent quenching, qE-quenching (Wraight and Crofts 1970), which is associated with the xanthophyll cycle pigments (Niyogi et al. 1998) and the regulatory protein of PSII, PsbS (Li et al. 2000). When light intensity is lowered, ΔpH collapses within 10–20 s (Ruban 2013, 2016), whereas NPQ is relaxed more slowly. The slow NPQ relaxation could limit photosynthesis in low light (LL) of fluctuating light (FL) (Zhu et al. 2004, Kromdijk et al. 2016).

Several studies have shown that FL causes PSI photoinhibition. We have reported significant PSI photoinhibition in wild-type (WT) *Arabidopsis thaliana* (Kono et al. 2014), *Oryza sativa* (Yamori et al. 2016) and some other field-grown plants (Kono et al. 2017). Large limitations on electron flow on the acceptor-

Plant Cell Physiol. 61(1): 192–202 (2020) doi:10.1093/pcp/pcz191, Advance Access publication on 16 October 2019,
available FREE online at https://academic.oup.com/pcp

side of PSI would cause damage to PSI, because of the accumulation of reactive oxygen species (Sonoike 1996, Takagi et al. 2016). Alternative photosynthetic electron flows, such as the CEF-PSI, have been proposed to contribute to the protection of PSI against FL (Suorsa et al. 2012, Kono et al. 2014, Yamori et al. 2016). As we recently reported, the addition of FR, at levels realistic to those in nature, to red FL suppresses PSI photoinhibition almost completely in the *A. thaliana* WT and some other plants (Kono et al. 2017). Thus, PSI photoinhibition because of FL may not be a serious problem in nature.

The roles of FR in photosynthesis have not been studied intensively. This is probably because monochromatic FR drives neither photosynthetic O_2 evolution nor CO_2 assimilation, and thereby FR is not included in PAR. Obviously, the primary role of FR is to oxidize P700 (Arnon et al. 1967, Myers 1971). FR alleviates acceptor-side limitations and imposes donor-side limitations on the electron flow in PSI, and thereby increases the fraction of oxidized P700, ($P700^+$)/(total P700). In this study, we assessed the effects of FR on CO_2 assimilation and the photosynthetic electron transport system in FL with HL and LL phases at a photosynthetic photon flux density (PPFD) of 800/30 μmol m^{-2} s^{-1} for 10/15 min. To avoid the complexities brought about by activation of various photosynthetic reactions and gradual stomatal opening, we used leaves that had been activated in moderate light at 135 μmol m^{-2} s^{-1} for about 30–60 min in all the measurements. Measurements were mostly taken from attached, intact leaves of the *A. thaliana* WT 'Col-0' but also from those of typical sun and shade plants. Furthermore, the effects of FR on the electron transport limitations in PSI were examined in natural sunlight.

Results

FR accelerated photosynthesis in the LL phase of the FL

We used light-emitting diodes (LEDs) that peaked at 740 nm (see **Supplementary Fig. S1** for the spectrum) for FR. For the moderate FR (m-FR) at 10.3 W m^{-2}, energy levels and PFDs in the 680–700 nm and 700–720 nm wavebands were 0.043 W m^{-2} and 0.2 μmol m^{-2} s^{-1}, and 1.7 W m^{-2} and 9 μmol m^{-2} s^{-1}, respectively. We assumed that about 5% of photons from the FR were absorbed by PSI pigments according to the absorptance spectrum in Hogewoning et al. (2012). The amount of photons absorbed by PSII pigments would be very small (**Supplementary Fig. S2**). For the actinic light (AL), red LEDs that peaked at 626 nm were used. We assumed that about 90% of photons of this AL were absorbed by photosynthetic pigments and that their energy was equally allocated to PSI and PSII.

Fig. 1 shows the effects of FR on the redox state of P700 in low AL at a PPFD of 30 μmol m^{-2} s^{-1} (LL) in *A. thaliana* 'Col-0' leaf. The leaf was first pretreated in the dark. After a series of measurements, the same leaf was kept in the light at 135 μmol m^{-2} s^{-1} for 60 min to fully activate the photosynthetic components and another series of measurements were taken. In both measurements, the first FR illumination oxidized a large proportion of P700 [high ($P700^+$)/(total P700)] and the P700

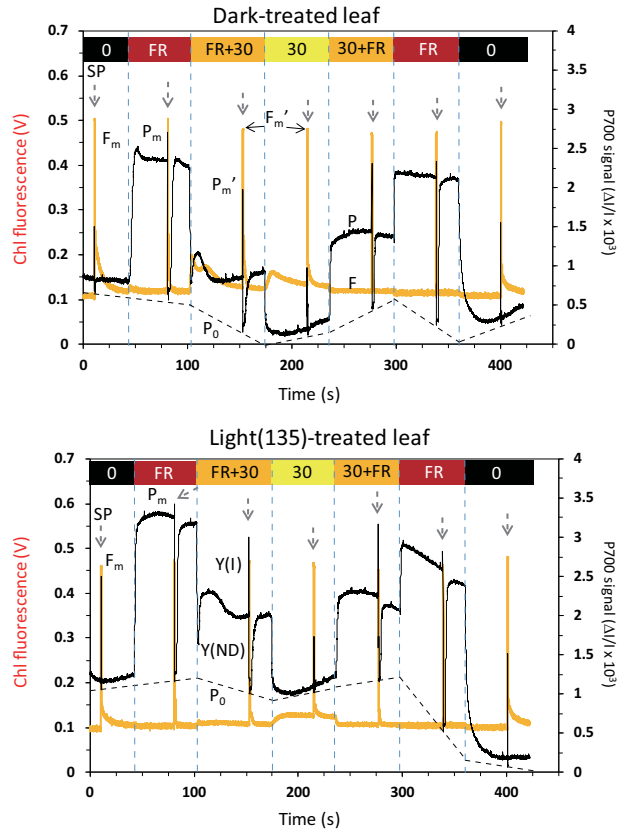

Fig. 1 Changes in Chl fluorescence (orange) and redox state of P700 (black) in successive illumination with FR, FR + LL and LL after a dark treatment (upper) and after a subsequent light treatment (lower) in a leaf of an *Arabidopsis thaliana* 'Col-0 plant'. The dark treatment for 60 min was followed by the first FR illumination. After the first set of measurements (upper figure), the leaf was subjected to light treatment at 135 μmol s m^{-2} s^{-1} for 60 min. After the 30-s dark period, the second set of measurements was taken (lower figure). During the measurements, we checked the basal level corresponding to the full reduction of P700, P_0, by applying a SP and subsequently the complete darkness. The dotted line shows the changes in the P_0 levels. FR at 10.3 W m^{-2} and LL at 30 μmol m^{-2} s^{-1} were from FR LEDs and red LEDs. Each dashed arrow denotes SP. F', F_m and F_m'; the Chl fluorescence level in the AL, and the maximum level with closed PSII centers in the dark and AL, P and P_0; P700 absorbance at given AL and level of the P700 full reduction. P_m and P_m', maximum oxidizable P700 in the dark and AL, respectively. The black, dark red, orange and yellow bars denote, dark, FR, LL + FR and LL, respectively. The CO_2 and O_2 partial pressures were 40 Pa and 20 kPa, respectively. Measurements were conducted in three leaves and typical traces using the same leaf are shown.

redox level attained a steady state. On the basis of the above assumptions, the actual electron flow rate through PSI was small (~2 μmol m^{-2} s^{-1}) because of the large NPQ by $P700^+$. When LL was added to FR (LL + FR), P700 was reduced by the electrons from PSII, but about 30–50% of P700 remained as $P700^+$. When FR was turned off (LL − FR), P700 was almost entirely reduced, indicating that the acceptor-side limitation of PSI, Y(NA), calculated as ($P_m - P_m'$)/P_m, increased. The quantum yield of PSI photochemistry, Y(I), calculated as ($P_m' - P$)/P_m, was about 0.6 in LL + FR and about 0.5 in LL − FR. This indicates that the higher Y(I) in LL + FR was achieved by

balancing Y(NA) and the donor-side limitation of PSI, Y(ND), calculated as $(P - P_0)/P_m$. The activation of photosynthesis by the light pre-treatment affected the transients of the Chl fluorescence trace upon addition and turning off of FR, but the activation exerted no marked effects on the redox state of P700.

Changes in the rate of net CO_2 assimilation and PSI and PSII parameters in leaves of WT *A. thaliana* 'Col-0' were measured in the FL, in which HL at 800 μmol m^{-2} s^{-1} for 10 min and LL at 30 μmol m^{-2} s^{-1} for 15 min alternated in the absence or presence of FR (**Fig. 2**). These FL treatments are expressed as FL-800/30 and FL-(800 + FR)/(30 + FR), where FR was added continuously to FL. As shown in **Supplementary Fig. S2**, when solely applied, this FR increased the CO_2 assimilation rate (Pn) by 0.13 ± 0.025 μmol m^{-2} s^{-1}. Therefore, subtracted 0.13 μmol m^{-2} s^{-1} from the Pn values obtained in the presence of FR and these 'corrected' values are shown in **Fig. 2A, B**. Upon the transition from HL to LL, Pn rapidly decreased for the first 30 s and then gradually increased to attain a steady state. In LL + FR, the decrease in Pn was slower than that in LL − FR. Pn at 5, 10 and 15 s from the onset of LL was significantly greater in LL + FR than in LL − FR (**Fig. 2A**), indicating the greater CO_2 assimilation in LL + FR after -HL illumination. From 300 s to 900 s after the onset of LL, the steady-state level of the corrected Pn for LL + FR was higher by 0.19 ± 0.007 μmol m^{-2} s^{-1} (mean ± SD, $n = 6$) than Pn in LL − FR (**Fig. 2B**). Upon the transition from the dark to HL, or LL to HL, Pn increased rapidly for the first 60 s and then gradually stabilized. Effects of FR were not apparent in HL conditions.

The NPQ of the Chl fluorescence in PSII was higher in HL than in LL. At least two components were involved in the decreased NPQ in LL. NPQ rapidly decreased for the first 180 s (fast phase) and thereafter slowed to a steady-state level from 180 s to 900 s after the onset of LL (slow phase). FR markedly accelerated the relaxation of NPQ (**Fig. 2E**). At 10 s after the shift to LL + FR, NPQ was close to the level at 40 s after the shift to LL − FR. In the slow phase, FR further relaxed NPQ to nearly 0.10, whereas the steady-state level was 0.31 in LL − FR. NPQ in HL showed a transient spike immediately after each shift to HL and FR had no effect on the steady-state values. Upon the shift from HL to LL, the quantum yield of PSII photochemistry(Y(II)), and the fraction of open PSII centers (qL), rapidly increased at first (fast phase) and then gradually attained their steady-state values (slow phase). The increases in Y(II) and qL were slower and the steady-state values were significantly lower in LL − FR than in LL + FR (**Fig. 2C, G**). From 180 to 900 s after the onset of LL, the difference in Y(II) between LL ± FR was 0.10 ± 0.005 (mean ± SD, $n = 6$). In HL, FR did not show any effect on Y(II) or qL.

On the basis of the results shown in **Fig. 2**, we hypothesized that FR enhanced photosynthesis in the LL phases of FL by rapidly relaxing qE-quenching. Thus, we tested this hypothesis by analyzing the *npq1 and npq4* mutants (**Supplementary Figs. S3, S4**). The *npq1* mutant is defective in violaxanthin de-epoxidase (VDE) and thus lacks zeaxanthin, and the *npq4* mutant is defective in PsbS, the regulatory protein of PSII. Although relaxation of NPQ in the *npq1* mutant showed the fast and slow phases similar to those in the WT, their absolute levels were low (**Supplementary Fig. S3**). The NPQ kinetics of *npq4* mutants in LL differed from those in *npq1*. Upon the transition to LL, NPQ in *npq4* transiently increased and then gradually decreased (**Supplementary Fig. S4**). In these mutants, the extent of NPQ relaxation in the fast phase was lower than that of the WT, and the differences in Y(II) and qL between +FR and −FR were reduced. These results indicate that, in the WT, FR accelerated the relaxation of the qE-quenching, resulting in higher Y (II) and qL in LL.

In HL, Y(ND) was high irrespective of exposure to FR. Upon the transition from HL − FR to LL − FR, Y(ND) rapidly decreased to almost zero (**Fig. 2F**, see also **Supplementary Fig. S5A**, C). When FR was present, Y(ND) decreased upon the transition to LL, but rapidly increased to 0.3 after that (**Fig. 2F**, see also **Supplementary Fig. S5B** and D). In HL ± FR, Y(NA) was lower than Y(ND). Y(NA) was somewhat lower in LL + FR than in HL + FR (**Fig. 2H**). In contrast, in LL − FR, Y(NA) gradually increased, then reached a plateau. Y(I) promptly reached a constant level upon the transition to LL + FR, whereas in LL − FR, Y(I) showed a prompt increase and then a gradual decrease, reaching a plateau, which complemented the changes in Y(NA) (**Fig. 2D**).

The light response curves of the steady-state values of Pn, Y (ND), Y(NA), Y(II) and NPQ at various PPFDs ranged from 1200 to 0 μmol m^{-2} s^{-1} with and without FR (**Supplementary Fig. S6**). In continuous light below 60 μmol m^{-2} s^{-1}, addition of FR decreased Y(NA) and increased Y(ND). However, it was insufficient to increase Pn significantly. At PPFDs below 60 μmol m^{-2} s^{-1}, Y(II) was significantly greater in the presence of FR, but neither the differences in Pn nor those in NPQ were significant. The difference in Y(II) between ±FR in LL at 30 μmol m^{-2} s^{-1} was 0.023, which was much smaller than the difference of 0.1 observed in FL.

Next, we confirmed whether FR independently affected the fast- or slow-phases of NPQ relaxation (**Fig. 3**). When FR was turned off for the first 180 s in the LL phase, NPQ relaxation decelerated. When FR was subsequently turned on after 180 s in the LL − FR phase, NPQ rapidly relaxed to nearly 0.1 in the slow phase. Y(II) also rapidly increased after adding FR at 180 s (**Fig. 3A**). Conversely, when FR was present for the first 180 s in LL, then turned off after 180 s, the NPQ relaxation stopped and NPQ remained at about 0.25 in the slow phase (**Fig. 3B**). The rapid increase in Y(II) was also retarded after FR was turned off. These clearly indicated that FR independently accelerated the fast- and slow-phase relaxation of NPQ. The redox state of PSI also changed depending on the presence or absence of FR in the LL phase in the same manner as shown in **Fig. 2** (**Supplementary Fig. S7**).

The effects of FR intensity on NPQ and Y(II) were examined (**Fig. 4**). Upon the shift to LL, either of four FR levels, null (−FR), low (l-FR), m-FR or high FR (h-FR) at 0, 3.5, 10.3 or 25.6 W m^{-2}, respectively, were applied. In the HL phase, m-FR was present unless otherwise stated. The dose-dependence of FR was seen in accelerating the NPQ relaxation and Y(II) increase (**Fig. 4A, C**). In the fast phase, NPQ relaxed more rapidly at higher FR intensity. In the slow phase, the addition of m-FR was sufficient for NPQ to relax to almost zero. Y(II) at 10 s from the onset of LL was significantly higher with h-FR than with m-FR. Thereafter,

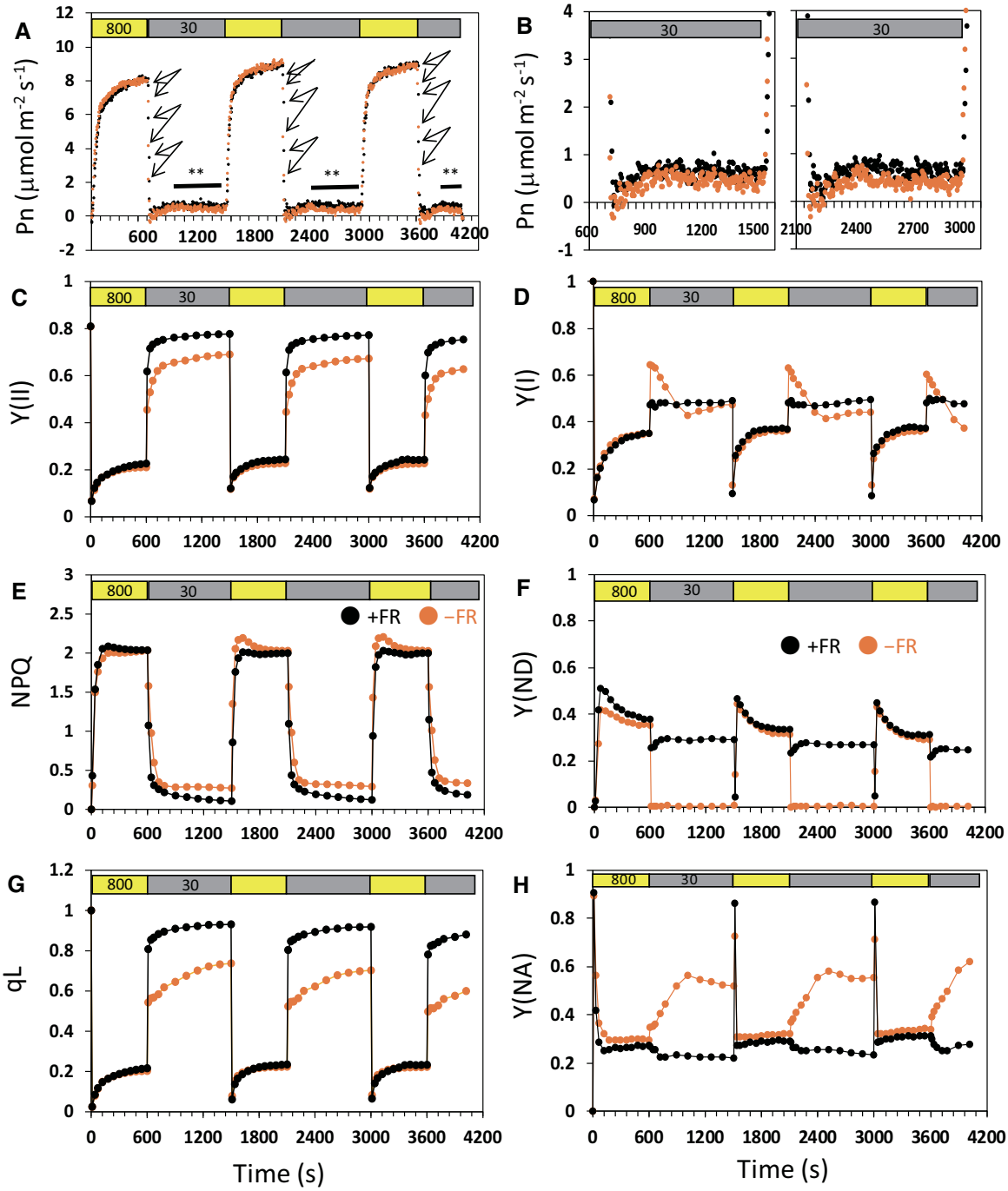

Fig. 2 Changes in the CO_2 assimilation rate, Pn, (A and B), PSII parameters (C, E and G) and PSI parameters (D, F and H) to the FL in *Arabidopsis thaliana* 'Col-0' leaves in the absence (FL-800/30, ●) and presence [FL-(800 + FR)/(30 + FR), ●] of m-FR. The FL was applied to the leaf which had been in the light at 135 μmol m^{-2} s^{-1} for 30–40 min and subsequently kept in the dark for 5 min. Pn values in the FL-(800 + FR)/(30 + FR) were corrected by subtracting 0.13 μmol m^{-2} s^{-1}, corresponding to the increase in Pn by just adding FR in the absence of AL (**supplementary Fig. S2**). In (A), each pair of arrows shows the difference between the rates measured with FR and without FR at 5, 10 or 15 s from the onset of LL. These differences were statistically significant by Student's *t*-test ($P < 0.05$). Asterisks (**) indicate significant differences between the mean rates for the LL period, which are averaged from 300 to 900 s for the first and second LL phases and from 300 to 600 s for the third LL phase ($P < 0.01$, paired *t*-test). Two panels in (B) are enlarged views of the first and second LL phases of (A). The leaf lamina was sandwiched in a chamber. The CO_2 and O_2 partial pressures were 40 Pa and 20 kPa, respectively. Each data point represents the mean ($n = 6$). Error bars are omitted for simplicity. Each of the leaves was used for the measurements with and without FR. The order of these two measurements was randomly chosen. For the error levels, see **Figs. 3, 4, 6**.

the differences between h- and m-FR were not seen. We also checked the response of Y(NA) because the effect of FR on the photosynthetic performance might be associated with its excitation of P700. FR suppressed Y(NA) in the LL phase, but the FR-intensity dependence was not observed in Y(NA) for the period corresponding to the fast phase of NPQ relaxation

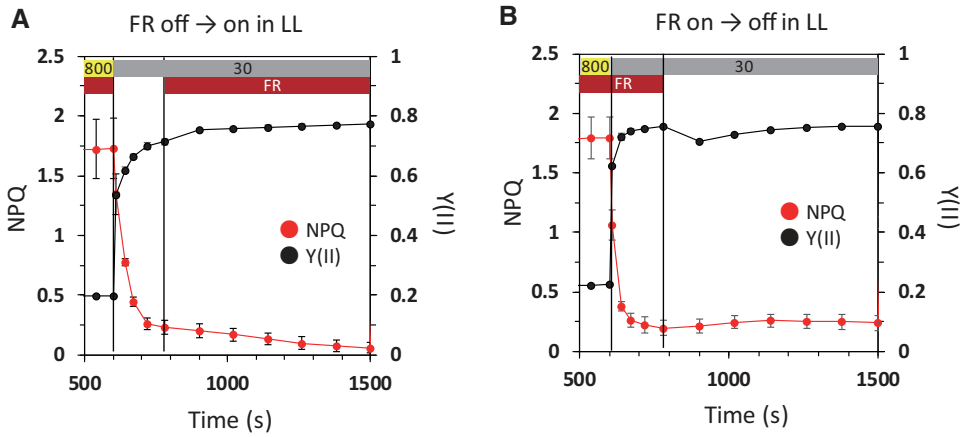

Fig. 3 Effects of FR on the fast- and slow relaxation of NPQ and the Y(II) increase in the LL phase of FL. (A) In the first 180 s of LL, FR was turned off, and then FR was turned on until the end of LL phase. (B) FR was turned off at 180 s after the beginning of LL. In HL, m-FR was present. Data for the last 2 min in HL (10 min) and 15 min in LL are shown. Yellow, gray and dark red bars denote HL, LL and FR, respectively. Measurements were made under the same conditions as those for **Fig. 2**. Each data point represents the mean ± SD ($n = 3$).

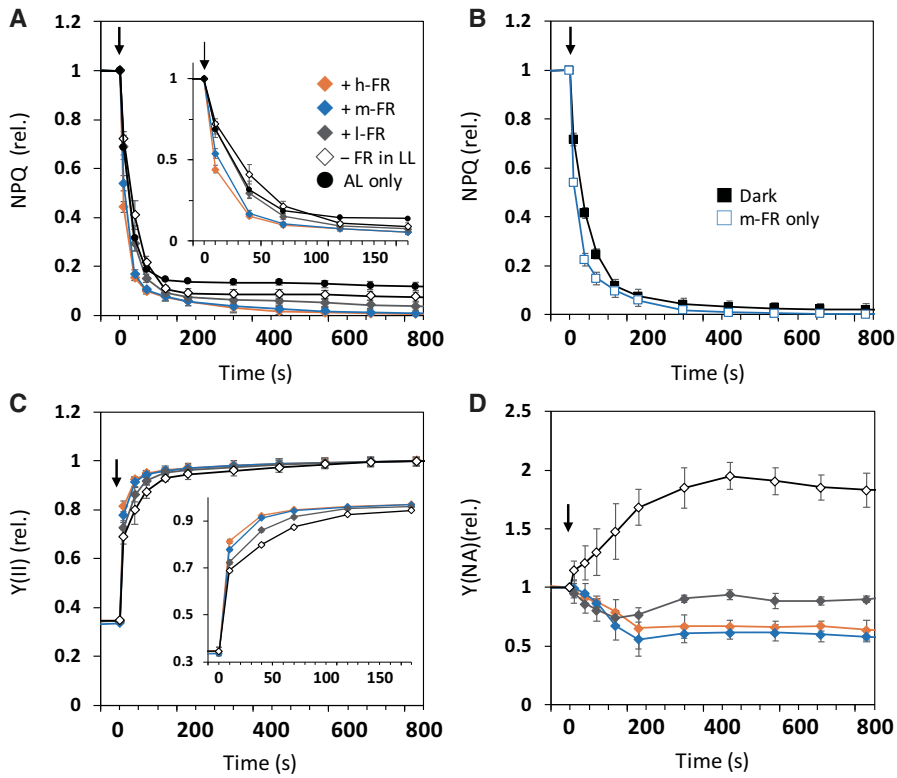

Fig. 4 Effects of the intensity of FR in LL on the NPQ relaxation (A and B), Y(II) (C) and Y(NA) (D) upon the shift from HL to LL. Four FR levels, h-FR, m-FR, l-FR and −FR, at 25.6, 10.3, 3.47 and 0 W m^{-2}, respectively, were used in LL. HL and LL were supplemented with FR as follows: ◆, (HL + m-FR)/(LL + h-FR); ◆, (HL + m-FR)/(LL + m-FR); ◆, (HL + m-FR)/(LL + l-FR); ◇, (HL + m-FR)/LL; ●, HL/LL; ■, (HL + m-FR)/Dark; and □, (HL + m-FR)/m-FR. Arrows show the shifts from HL to LL (or darkness). Data were taken from the first shifts from HL (from the last 1 min) to LL. Zero seconds on the *x*-axis denotes the beginning of LL. Insets in (A) and (C) are the enlarged views for 180 s after the shift to the LL phase. The data of NPQ and Y(NA) were normalized to the value at the end of the HL phase. The data of Y(II) were normalized to the value at the end of the LL phase. Measurements were taken under the same conditions as for **Fig. 2**. Each data point represents the mean ± SD ($n = 3$).

(**Fig. 4D**). In contrast, in the slow phase of NPQ relaxation, m-FR and h-FR decreased Y(NA) to similar levels. These results indicate that FR accelerated NPQ relaxation and Y(II) increase after the transition to LL in an intensity-dependent manner.

NPQ relaxation was faster in m-FR (in the absence of LL) than in the dark (**Fig. 4B**). Interestingly, the presence of FR in the HL phase facilitated NPQ relaxation in the slow phase in LL even when LL contained no FR (compare ◇ and ● in

Fig. 4A). This suggests that FR exerted some effects in HL as well.

Effect of FR on *pmf*

Acceleration of Pn and PSII electron transfer in LL could be related to the proton transfer across the thylakoid membrane. To examine the effect of FR on the *pmf*, we analyzed the dark-interval relaxation kinetics (DIRK) transient of the carotenoid electrochromic shift (ECS) after turning off the AL. Fig. 5A shows the DIRK traces in the leaves analyzed after turning off the LL at 30 μmol m^{-2} s^{-1} and m-FR at 40, 120 and 300 s after the transition from HL at 800 μmol m^{-2} s^{-1} ±FR to LL±FR. The ECS transients obtained by turning off the LL − FR at 300 s showed a typical trace: a rapid decline upon turning off the red AL and a subsequent slow rise to a steady-state level. However, the ECS transients after LL + FR for 300 s markedly differed. The rapid decline of the signal upon turning off both AL and FR was followed by a slower decline for about 5 s and a subsequent rise to an apparent steady state. The traces obtained at 40 s and 120 s after the LL were similar, although the drifts in the latter transients were considerable.

To characterize the effects of FR on the flux(es) of ion(s) across the thylakoid membrane, we followed the conventional method and estimated the total *pmf* from the amplitude of the rapid decline of the ECS upon turning the light off, tentatively ignoring the slow decay (Fig. 5B). The total *pmf* thus estimated was attributed to the proton efflux via the thylakoidal H^+-ATPase. The total *pmf* levels were similar at 40 s and 120 s but lower at 300 s. The effects of FR were not apparent. H^+ conductance (g_H^+), which is used to express the conductivity of the thylakoid membrane to protons, determined predominantly by the flux through the H^+-ATPase, however, was significantly greater with FR than without FR. The magnitude of g_H^+ was unchanged with time. The initial rate of the decay of the ECS signal (vH^+), which is used as an estimate of the relative flux of protons through the H^+-ATPase, was also greater with FR.

Effects of FR in LL phase on NPQ relaxation in various levels of FL

The effects of PPFD levels of HL at 2000, 800 and 300 μmol m^{-2} s^{-1} and/or LL at 200 and 30 μmol m^{-2} s^{-1} on NPQ relaxation upon the transition to LL were examined (Fig. 6). In HL, m-FR was present. In FL-2000/30, both the fast and slow phases of NPQ relaxation in LL were accelerated by FR (Fig. 6A). Similarly, the Y(II) recovery accelerated with increasing FR intensity. The NPQ relaxation in FL-2000/30 was slower than that of FL-800/30 (Fig. 4). Moreover, even in the presence of m-FR, NPQ did not decline to zero. On the contrary, in FL-300/30, the NPQ relaxation in the fast phase was slower in the presence of FR than in its absence (Fig. 6G), whereas the Y(II) increase was faster (Fig. 6H). In the slow phase, from 180 to 900 s, NPQ relaxation was faster in LL + FR, whereas, in LL − FR, the decline was not observed. In FL-2000/200 and FL-800/200, the addition of FR hardly accelerated the NPQ relaxation and Y(II) recovery (Fig. 6C–F).

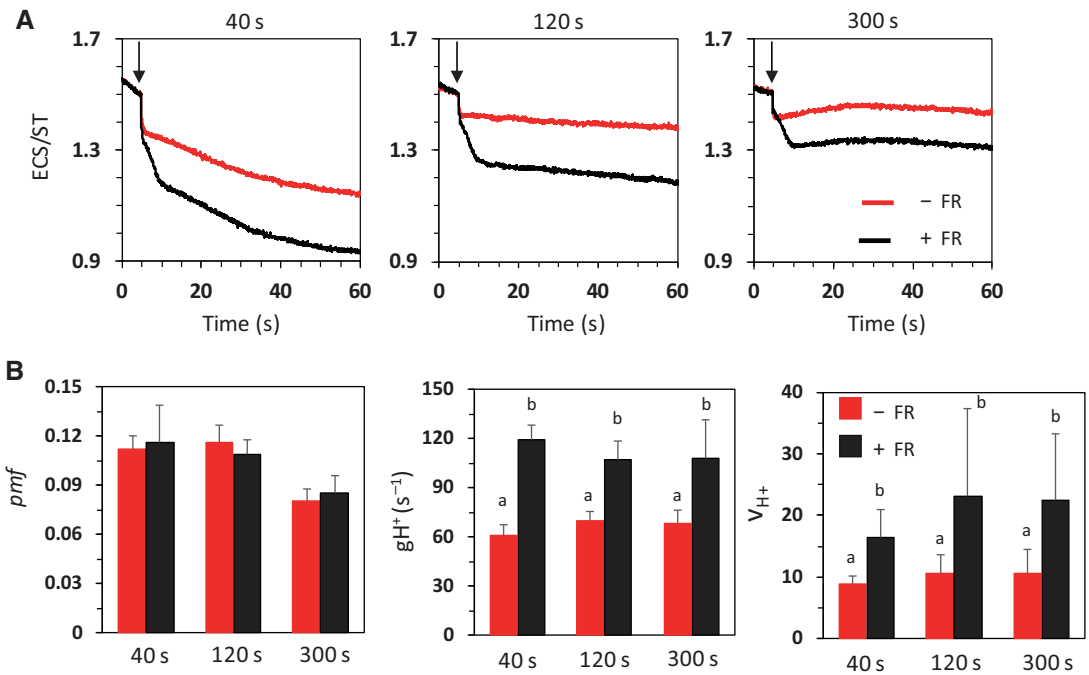

Fig. 5 The DIRK of the ECS signal measured in the leaves. (A) The DIRK of ECS signals at 40 (left), 120 (middle) and 300 s (right) after the onset of LL (30 μmolm^{-2} s^{-1}) ±m-FR at 10.3 W m^{-2}. Leaves, which had been kept at 135 μmol m^{-2} s^{-1} for 40 min, were treated in HL ± m-FR for 10 min and then in LL ± m-FR. Arrows indicate the AL (and FR) light off. (B) The total *pmf*, proton conductivity (g_H^+) and the initial rate (vH^+) estimated from ECS changes in A. g_H^+ and vH^+ were calculated as the inverse of a decay time constant and the initial slope of the ECS decay for a 100–200 ms dark period, respectively. ECS signals were normalized by a single-turnover flash. The CO_2 and O_2 partial pressures were 40 Pa and 20 kPa, respectively. The values represent the mean ± SD ($n = 3–5$). Different lower-case letters indicate statistically significant differences ($P < 0.05$).

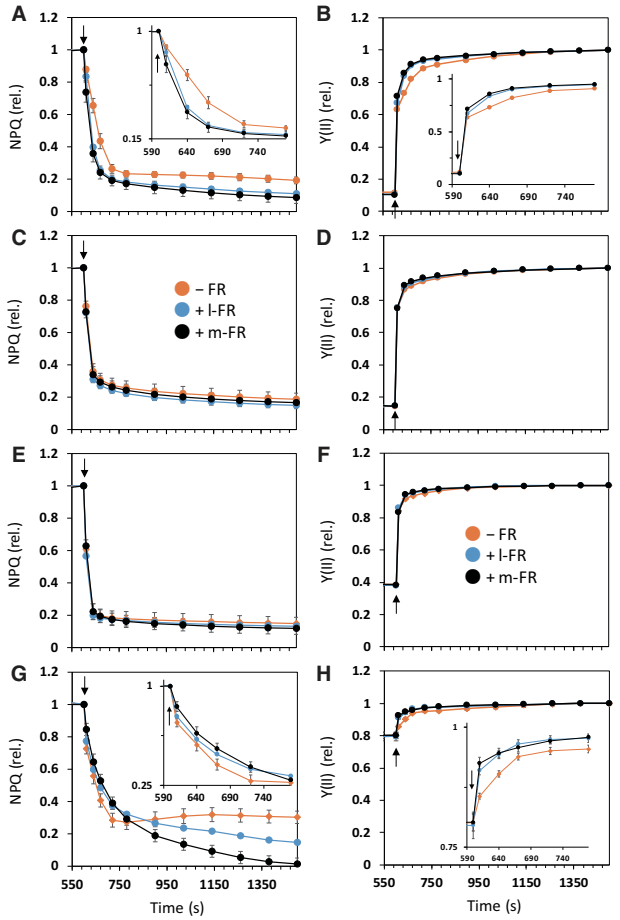

Figure 6. Effects of the FR intensity on NPQ relaxation (A, C, E and G) and Y(II) recovery (B, D, F and H) in LL in various FLs. ●, −FR; ●, +l-FR; ●, +m-FR. The leaves that had been kept at 135 μmol m^{-2} s^{-1} for 40 min were treated in HL and then LL. HL/LL conditions were: (A and B) (2000 + m-FR)/(30 + x-FR); (C and D) (2000 + m-FR)/(200 + x-FR); (E and F) (800 + m-FR)/(200 + x-FR) and (G and H) (300 + m-FR)/(30 + x-FR). Arrows show the timing of the shift from HL to LL. Insets show the enlarged views for 180 s from the transition to LL phase. The mean values of NPQ for these HL + m-FR treatments were 2.00 in HL at 2000 μmol m^{-2} s^{-1}, 1.78 in HL at 800 μmol s m^{-2} s^{-1} and 0.43 in HL at 300 μmol m^{-2} s^{-1}, respectively. The data of NPQ and Y (II) were normalized by the value at the end of HL and LL, respectively. Measurements were taken under the same conditions as those in **Fig. 2**. Each data point represents the mean ± SD ($n = 3$).

Relevance of the present observations in other species and under field conditions

We also conducted measurements, similar to those shown in **Fig. 2**, in *Nicotiana tabacum*, a sun species, and in *Alocasia odora*, a shade tolerant species. According to their required light conditions for growth, we chose different PPFD levels for HL and LL (see **Supplementary Figs. S5E–H, S8, S9**). The results obtained with *A. thaliana* were largely reproducible in these species, namely that typical sun and shade plants also showed the effect of FR on photosynthetic performance.

To compare the intensities of FR used in this study and those in the field, we measured PFD over a range of 400–780 nm in an open site and on the floor of a broad-leaved deciduous forest. In the open site, PFD of FR (700–780 nm), around noon, attained about 500 μmol m^{-2} s^{-1} on sunny days, whereas PFD of FR (700–780 nm) on the forest floor ranged from 20 to 50 μmol m^{-2} s^{-1} (**Supplementary Fig. S10**). On the forest floor, the PFD of FR was always greater than that of red light (600–700 nm). These results indicate not only that the FR intensities used in this study were appropriate, but also that the presence of FR is of importance in the consideration of photosynthesis in the field.

Whether FR in the field contributes to the oxidation of P700 was examined by eliminating FR using an infra-red cut-off filter. The *A. thaliana* plants were placed in an open site, and the 830 nm waveband and Chl fluorescence signals were monitored. Although the presence and absence of the FR (>700 nm) did not affect the response of the Chl fluorescence, the P700 signal detected as the 830 nm reflectance clearly decreased upon the elimination of FR. When FR was turned off, Y(ND) decreased and Y(NA) increased. This result indicates that, under these field conditions, FR contributed to the increase in the fraction of $P700^+$ (**Supplementary Fig. S11**).

Discussion

FR (>700 nm) hardly drives photosynthetic O_2 evolution and CO_2 assimilation. Here, we examined the effect of FR on photosynthesis in FL, and the results are summarized as follows: (i) in low AL, FR released the acceptor-side limitation on PSI and simultaneously imposed the donor-side limitation on PSI (**Figs. 1, 2, 4**); (ii) FR enhanced CO_2 assimilation after the transition from HL to LL in the FL by accelerating both NPQ relaxation and Y(II) increase, probably because of acceleration of ΔpH dissipation by FR (**Figs. 2, 3, 5**); (iii) the acceleration of NPQ relaxation by FR occurred when the PPFD level in the LL phase was low and that in the HL phase was sufficiently high (**Fig. 6**); and (iv) similar results were obtained in *N. tabacum* and *A. odora* (Supplementary Figs. S8, S9).

When FR was given solely, it induced an increase in the oxidized P700 fraction [($P700^+$)/(total P700)], whereas P700 was almost completely reduced in low AL (Asada et al. 1992, **Fig. 1**). Addition of FR to low AL in FL increased the ($P700^+$)/(total P700) ratio to a relatively high level. However, the NPQ by $P700^+$ limited neither Y(I) nor Y(II). In contrast, in the absence of FR, the steady-state level of Y(II) in LL gradually decreased with the FL cycle (**Fig. 2C**). Moreover, large limitation of the PSI acceptor-side in low AL could lead to PSI photoinhibition upon a sudden increase in PPFD (Kono et al. 2017). Thus, it appears that the maintenance of some oxidized P700 contributes to the well-balanced photosynthesis in FL (Joliot and Joliot 2006, Laisk et al. 2010, Miyake 2010, Kono et al. 2017, Takagi et al. 2017).

FR drives CEF-PSI, when it is given solely (Miyake et al. 1995). However, because the high activity of CEF-PSI inevitably limits the LEF, if the rate of CEF-PSI induced by FR were high, Y(II) in LL + FR would be smaller than that in LL − FR. In reality, Y(II) was greater in LL + FR, although FR per se did not drive PSII (**Fig. 2** and **Supplementary Fig. S6**). Therefore, the electrons

ejected from PSI by FR contributed more to linear electron transport and CO_2 assimilation. Enhancement of Pn would require more ATP synthesis, which might be supported by the higher gH^+ in LL + FR than in LL − FR (**Fig. 5**). In this study, however, we did not try to separate *pmf* into ΔpH and ΔΨ in the way proposed by Sacksteder et al. (2000) and Cruz et al. (2001) because the DIRK after LL + FR showed the second decay. Further investigations of the nature of the second decay are required.

When the irradiance suddenly drops, the decrease in Pn delays for several seconds, and thus the CO_2 assimilation for the cumulative irradiance is greater than that calculated based on the steady-state rates under continuous light conditions (Kirschbaum and Pearcy 1988, Pons and Pearcy 1992, Roden and Pearcy 1993, Pearcy et al. 1996, Kirschbaum et al. 1998). FR enhanced the post-illumination CO_2 assimilation for about 20 s after the shift from HL to LL (**Fig. 2**). In LL soon after HL, the reducing power and the pools of RuBP and triose-phosphates that accumulates in HL (Laisk et al. 1987) are used in the post-illumination CO_2 assimilation (Pearcy 1990). The post-illumination CO_2 assimilation also requires ATP (Hangarter and Good 1982, Laisk et al. 1984, Sharkey et al. 1986, Pearcy 1990). High gH^+ and vH^+ in LL + FR (**Fig. 5**) could reflect the higher rate of ATP synthesis.

The prompt regulation of NPQ is a potent strategy for improving photosynthesis in FL. When the irradiance drops, the relaxation of NPQ is considerably delayed (Pérez-Bueno et al. 2008). Thus, after the shift to LL, NPQ transiently limits CO_2 assimilation. In a modelling study of canopy photosynthesis of total diurnal carbon loss because of the slow relaxation of NPQ was estimated to be 13–32% lower than that of NPQ relaxation without delay, upon the rapid change in the PPFD (Zhu et al. 2004). Recently, aiming at suppressing NPQ limitation, transgenic *N. tabacum* lines overexpressing VDE, zeaxanthin epoxidase and PsbS were created (Kromdijk et al. 2016). These plants clearly showed faster NPQ relaxation and higher Pn upon the PPFD drop than that of the WT. Here, we showed in the WT that FR enhanced CO_2 assimilation in the LL phase of FL by accelerating NPQ relaxation. Using *npq* mutants, we found that FR accelerated the relaxation of the qE-quenching, resulting in higher Y(II) in LL to some extent (**Supplementary Figs. S3, S4**).

Analyses of the *npq* mutants provided further insight into the efficient response to the FL. In LL ± FR, Y(II) was higher in the *npq* mutants than in the WT plant, suggesting that the qE-quenching induced in HL limits photosynthesis in the next LL phase in WT plants. In LL, the steady-state Y(I) in the WT did not differ, irrespective of FR, but the steady-state Y(I) in the *npq* mutants was much lower in LL−FR than in LL + FR. This indicates that qE-quenching is required to balance the LEF in FL, especially in the absence of FR. On the contrary, the improvement of Y(I) in LL + FR indicates that FR is needed to balance photosynthesis in FL, especially in the *npq* mutants.

FR intensities used in this study were similar to the levels observed in the open field site and understory (**Supplementary Fig. S10**). We also confirmed the FR effects in the FL in typical sun- and shade-type plants (**Supplementary Figs. S8, S9**). Furthermore, we examined the effects of FR elimination on P700 excitation in the natural sunlight (**Supplementary Fig. S11**). These results indicate that the present findings are general and relevant in the field.

In contrast to LL, the effects of FR on Pn and PSII and PSI photochemistry were not apparent in the HL phases FL (**Fig. 2**) or in the continuous light at high PPFD levels (**Supplementary Fig. S6**) in the *A. thaliana* plants. However, the NPQ relaxation in LL − FR was faster after HL + FR than after HL − FR (**Fig. 4A**). This implies that FR affected the electron transport system in HL to some extent, although its effect was not apparent in the HL phases of FL, probably because the absorbed FR level was less than the absorbed red AL. These observations were made in pre-illuminated, fully activated leaves. Photosynthetic induction is mainly limited by the activation of the RuBP regeneration processes, the Calvin–Benson cycle enzymes, such as Rubisco, and stomatal opening (Pearcy 1990, Way and Pearcy 2012, Kaiser et. al. 2015). We also measured the induction response of Pn to a sudden increase in PPFD in the dark-treated leaves, in which the Calvin–Benson cycle was inactivate and the stomata were closed. The induction curves of Pn upon illumination with red AL at 800 μmol m^{-2} s^{-1} for 30 min were similar irrespective of the presence or absence of FR (**Supplementary Fig. S12**). Thus, FR may not affect the photosynthetic induction processes.

In *N. tabacum* (**Supplementary Fig. S8**) and *A. odora* (**Supplementary Fig. S9**), Pn in the HL phases of FL was also higher with FR than without FR. This implies that whether the effects of FR in HL are apparent would depend on the species, growth light, and FL conditions, such as the PFD levels of PAR and FR. For more general trends of the FR-effects, more detailed studies are needed. For the next step, we should confirm whether the FR-effect on the acceleration of photosynthesis and the NPQ relaxation is adaptive under field conditions.

In this study, we showed that the plants exposed to FL photosynthesized well in the presence of FR by accelerating the NPQ relaxation and Y(II) increase, which was probably because of the increased gH^+, reflecting both faster ΔpH dissipation and faster ATP synthesis. Although further studies are needed to elucidate the detailed mechanism of the FR-effect, this study not only showed the importance of FR under FL conditions but also provided several seeds for future studies. We need to pay more attention to FR when we study photosynthetic performance. Elucidation of the exact mechanism of the FR-effect on photosynthesis is needed to truly understand plant performance in natural environments.

Materials and Methods

Plant materials

WT *A. thaliana* 'Col-0' plants were pot-grown in a growth chamber at 23 °C and relative humidity of 60%. In the 8-h photoperiod, light was provided by a bank of white fluorescent tubes and the irradiance at the plant level was 135 μmol m^{-2} s^{-1}. Plants were irrigated 2–3 times a week with deionized water for 2 weeks after germination, and afterwards with a 1 : 500 strength Hyponex 6–10-5 solution (Hyponex Japan). Mature rosette leaves from 7- to 10-week-old plants were used in experiments.

Arabidopsis thaliana mutants (*npq1*, Niyogi et al. 1998; *npq4*, Li et al. 2000) were grown under the same environmental conditions as the Col-0 plants. The *npq1* and *npq4* mutants are used in Supplementary Figs. S3, S4, respectively.

Nicotiana tabacum, a sun plant, was grown in a constant white light at 200 μmol m^{-2} s^{-1} in a growth chamber with an 8 h/16 h light/dark cycle. *Alocasia odora*, a shade plant, was grown in a constant white light at 60 μmol m^{-2} s^{-1} in a growth chamber with an 8 h/16 h light/dark cycle. Other environmental conditions were the same as those used for *A. thaliana* plants. *Nicotiana tabacum* and *A. odora* plants are used in Supplementary Figs. S8, S9, respectively.

FL and FR treatments

In this study, we used FL, in which HL at 800 μmol m^{-2} s^{-1} for 10 min and LL at 30 μmol m^{-2} s^{-1} for 15 min alternated. For both HL and LL, red LEDs with a wavelength peak at 630 nm were used. The FR, provided by LEDs with a wavelength peak at 740 nm, was at 10.3 W m^{-2} (m-FR). An integration of the spectrum shown in **Supplementary Fig. S1** gave 50.4 μmol m^{-2} s^{-1}. This was an appropriate level corresponding to those found in the field. FR was constantly supplied throughout the FL treatments. When FR was used in combination with the actinic red light, the FL treatments are abbreviated such as FL-(800 + FR)/(30 + FR). In some experiments, high- and low FR at 25.6 (h-FR) and 3.47 (l-FR) W m^{-2}, corresponding to 126 and 15 μmol m^{-2} s^{-1} of PPFD, were used.

Gas exchange, Chl fluorescence and 830-nm absorbance change measurements

Gas exchange, Chl fluorescence and absorption changes at 830 nm were measured simultaneously in intact leaves in a Dual-PAM Gas-Exchange Cuvette (3010-Dual; Heinz Walz GmbH, Effeltrich, Germany) with a GFS-3000 (Portable Gas Exchange System; Walz, Effeltrich, Germany) and a DUAL-PAM-100 (Chl fluorescence and P700 absorption analyzer equipped with a P700 dual wavelength emitter at 830 and 875 nm; Walz, Effeltrich, Germany). The CO_2 concentration in the leaf chamber was regulated with the GFS-3000 Control Unit 3000-C. The O_2 concentration in the air was controlled by mixing N_2 gas and O_2 gas using mass flow controllers. The CO_2 and O_2 partial pressures in the leaf chamber were 40 Pa and 20 kPa, respectively. The leaf temperature was controlled at 23 °C. Vapor pressure deficit ranged from 0.6 to 0.75 kPa.

Saturation pulses (SPs) from red LEDs (7000 μmol m^{-2} s^{-1}, 400-ms duration) were applied to determine the maximum Chl fluorescence with closed PSII centers after a dark treatment (F_m) and in AL (F_m'). The maximum photochemical quantum yield of PSII (F_v/F_m) in the dark was calculated as $(F_m - F_0)/F_m$, where F_0 is the minimal Chl fluorescence yield in the dark. The effective quantum yield of PSII in AL, Y(II), was calculated as $(F_m' - F')/F_m'$, where F' is the Chl fluorescence level in the AL from red LEDs that peaked at 635 nm (Genty et al. 1989). The coefficient of photochemical quenching, qL, a measure of the fraction of open PSII reaction centers, based on the 'lake model' of PSII antenna pigment organization, was calculated as $(F_m' - F')/(F_m' - F_0')\times F_0'/F'$ (Kramer et al. 2004). F_0' is the minimal fluorescence yield in an AL and was estimated as $F_0/(F_v/F_m + F_0/F_m')$ according to Oxborough and Baker (1997). Two other PSII quantum yields, Y(NPQ) and Y(NO), which represent the regulated and non-regulated energy dissipation in PSII, respectively, were calculated as $F'/F_m' - F'/F_m$ and F'/F_m, respectively (Hendrickson et al. 2004). These add up to unity with the photochemical quantum yield [i.e. Y(II) + Y(NPQ) + Y(NO) = 1]; for details, see Klughammer and Schreiber (2008).

With the Dual-PAM-100, $P700^+$ was monitored as the absorption difference between 830 and 875 nm in transmission mode. In analogy to the quantum yields of PSII, the quantum yields of PSI were determined using the SP method (Klughammer and Schreiber 1994). For the P700 parameters, the following values were measured: P, P700 absorbance in AL, P_m, P_m', maximum oxidizable P700 levels in the dark and in AL, P_0, and the level of the P700 full reduction. P_m was determined by application of the SP in the presence of FR at 740 nm. As the decrease in P_m is an indicator of PSI photoinhibition, it needed to be determined. We checked the intensity of FR to obtain an optimal level of P_m. In the leaves light-treated at the growth PPFD of 135 μmol m^{-2} s^{-1}, we measured P_m in FR light at 25.6 W m^{-2}. In the dark-treated leaves, the FR used was at a lower intensity of 3.47 W m^{-2}. These observations might be related to the activation state of the Calvin–Benson cycle and the pool size of stromal components that accept the electrons from PSI by FR-dependent excitation of P700. Y(I), Y(ND) and Y(NA) were determined in the AL. These add up to unity with the photochemical quantum yield [i.e. Y(I) + Y(ND) + Y(NA) = 1]. To oxidize the intersystem electron carriers, we applied FR for 200 ms before the start of the SP until its cessation. When FR was added to the AL, the P700 absorbance signal showed some drift (Supplementary Figs. S5, S7C, D). This is observed with most of the DUAL-PAM systems. We routinely checked that P_0 and Y(ND) were correctly measured by the SP in the presence of FR (**Supplementary Fig. S13**). P_0 was obtained from the signal in the dark for 1000 ms after the SP for 400 ms. During the dark interval, all the lights, including red AL, FR and SP, were turned off.

Measurements were carried out in the light-adapted leaves at 135 μmol m^{-2} s^{-1} for 30–40 min to fully activate the Calvin–Benson cycle enzymes and to open the stomata. When the HL phase transferred to the LL phase, the SP was applied at 10, 40, 70, 120, 180, 300, 420, 540, 660, 780 and 900 s from the onset of LL. Upon the transfer from dark to HL, or from LL to HL, the SP was applied at 10, 40, 70, 120, 180, 240, 300, 360, 420, 480 and 600 s from the onset of HL. These are applicable to Figs. 2–4, 6.

Measurement of ECS signal

The *pmf* was assessed by measuring the electrochromic absorbance shift (ECS or P515) with the DUAL-PAM-100 using the P515/535 module. The ECS signal is the difference between the transmittance at 550 nm and that at 515 nm (Klughammer et al. 2013). For determinations of the rate of proton efflux via the H^+-ATPase (vH^+), the proton conductivity of the thylakoid membrane (g_H^+), (Joliot and Joliot 2002; Avenson et al. 2005) and the size of the *pmf* (Sacksteder et al. 2000; Cruz et al. 2001), DIRK-analysis was conducted [for details, see Baker et al. (2007)]. The ECS decay from the AL turn-off for 100–200 ms in the dark was fitted by one-component decay kinetics, $A_1e^{-k1t} + B$, where A_1 is an amplitude constant, k_1 is a rate constant and B is a constant. The rate of proton efflux via the H+-ATPase was calculated as A_1k_1. Proton conductivity of the thylakoid membrane was identical to k_1. ECS signals were normalized by a single-turnover flash for 10 μs.

Supplementary Data

Supplementary data are available at PCP online.

Funding

This work was supported by JSPS KAKENHI Grant Number 19K16162, 17H05718 and 19H04718.

Acknowledgments

We would like to thank Professor Ryo Matsuda (University of Tokyo) for helpful support with the DUAL-PAM-F and Krishna Niyogi (University of California) for providing us with the seeds of *npq1* and *npq4* mutants. We thank Dr Daisuke Takagi for helpful discussions. We also thank anonymous reviewers for their critical comments on the early versions of the manuscript.

Disclosures

The authors have no conflicts of interest to declare.

References

Adams, W.W., Demmig-Adams, B. and Winter, K. (1990) Relative contributions of zeaxanthin-related and zeaxanthin-unrelated types of 'high-energy-state' quenching of chlorophyll fluorescence in spinach leaves exposed to various environmental conditions. *Plant Physiol.* 92: 302–309.

Arnon, D.I., Tsujimoto, H.Y. and Mcswain, B.D. (1967) Ferredoxin and photosynthetic phosphorylation. *Nature* 214: 562–566.

Asada, K., Heber, U. and Schreiber, U. (1992) Pool size of electrons that can be donated to P700+ as determined in intact leaves: donation to P700+ from stromal components via the intersystem chain. *Plant Cell Physiol*. 33: 927–932.

Avenson, T.J., Cruz, J.A., Kanazawa, A. and Kramer, D.M. (2005) Regulating the proton budget of higher plant photosynthesis. *Proc. Natl. Acad. Sci. USA* 102: 9709–9713.

Baker, N.R., Harbinson, J. and Kramer, D.M. (2007) Determining the limitations and regulation of photosynthetic energy transduction in leaves. *Plant Cell Environ*. 30: 1107–1125.

Brody, M. and Emerson, R. (1959) The effect of wavelength intensity of light on the proportion of pigments in *Porphyridium cruentum*. *Am. J. Bot*. 46: 433.

Cruz, J.A., Sacksteder, C.A., Kanazawa, A. and Kramer, D.M. (2001) Contribution of electric field (ΔY) to steady-state transthylakoid proton motive force (pmf) in vitro and in vivo. Control of pmf parsing into ΔY and ΔpH by ionic strength. *Biochemistry* 40: 1226–1237.

Emerson, R., Chalmers, R. and Cederstrand, C. (1957) Some factors influencing the long-wave limit of photosynthesis. *Proc. Natl. Acad. Sci. USA* 43: 133–143.

Emerson, R. and Lewis, C.M. (1943) The dependence of the quantum yield of chlorella photosynthesis on wave length of light. *Am. J. Bot*. 30: 165–178.

Gates, D.M. (1980) Spectral characteristics of radiation and matter. *In* Biophysical Ecology. Edited by Reichle, D. E. pp. 181–267. Springer, New York, NY.

Genty, B., Briantais, J.M. and Baker, N.R. (1989) The relationship between the quantum yield of photosynthetic electron transport and quenching of chlorophyll fluorescence. *Biochim. Biophys. Acta* 990: 87–92.

Hangarter, R.P. and Good, N.E. (1982) Energy thresholds for ATP synthesis in chloroplasts. *Biochim. Biophys. Acta* 681: 397–404.

Hendrickson, L., Furbank, R.T. and Chow, W.S. (2004) A simple alternative approach to assessing the fate of absorbed light energy using chlorophyll fluorescence. *Photosynth. Res*. 82: 73–81.

Hogewoning, S.W., Wientjes, E., Douwstra, P., Trouwborst, G., van Ieperen, W., Croce, R., et al. (2012) Photosynthetic quantum yield dynamics: from photosystems to leaves. *Plant Cell* 24: 1921–1935.

Joliot, P. and Joliot, A. (2002) Cyclic electron transfer in plant leaf. *Proc. Natl. Acad. Sci. USA* 99: 10209–10214.

Joliot, P. and Joliot, A. (2005) Quantification of cyclic and linear flows in plants. *Proc. Natl. Acad. Sci. USA* 102: 4913–4918.

Joliot, P. and Joliot, A. (2006) Cyclic electron flow in C3 plants. *Biochim. Biophys. Acta* 1757: 362–368.

Kaiser, E., Morales, A., Harbinson, J., Kromdijk, J., Heuvelink, E. and Marcelis, L.F.M. (2015) Dynamic photosynthesis in different environmental conditions. *J. Exp. Bot*. 66: 2415–2426.

Kirschbaum, M.U.F., Küppers, M., Schneider, H., Giersch, C. and Noe, S. (1998) Modelling photosynthesis in fluctuating light with inclusion of stomatal conductance, biochemical activation and pools of key photosynthetic intermediates. *Planta* 204: 16–26.

Kirschbaum, M.U.F. and Pearcy, R.W. (1988) Concurrent measurements of oxygen- and carbon-dioxide exchange during lightflecks in *Alocasia macrorrhiza* (L.) G. Don. *Planta* 174: 527–533.

Klughammer, C. and Schreiber, U. (1994) An improved method, using saturating light-pulses, for the determination of photosystem-i quantum yield via P700+-absorbency changes at 830 nm. *Planta* 192: 261–268.

Klughammer, C. and Schreiber, U. (2008) Complementary PS II quantum yields calculated from simple fluorescence parameters measured by PAM fluorometry and the saturation pulse method. *PAM Appl. Notes* 1: 27–35.

Klughammer, C., Siebke, K. and Schreiber, U. (2013) Continuous ECS-indicated recording of the proton-motive charge flux in leaves. *Photosynth. Res.* 117: 471–487.

Kono, M., Noguchi, K. and Terashima, I. (2014) Roles of the cyclic electron flow around PSI (CEF-PSI) and O2-dependent alternative pathways in regulation of the photosynthetic electron flow in short-term fluctuating light in *Arabidopsis thaliana*. *Plant Cell Physiol*. 55: 990–1004.

Kono, M., Yamori, W., Suzuki, Y. and Terashima, I. (2017) Photoprotection of PSI by far-red light against the fluctuating light-induced photoinhibition in *Arabidopsis thaliana* and field-grown plants. *Plant Cell Physiol*. 58: 35–45.

Kramer, D.M., Johnson, G., Kiirats, O. and Edwards, G.E. (2004) New flux parameters for the determination of QA redox state and excitation fluxes. *Photosynth. Res*. 79: 209–218.

Kramer, D.M. and Sacksteder, C.A. (1998) A diffused-optics flash kinetic spectrophotometer (DOFS) for measurements of absorbance changes in intact plants in the steady-state. *Photosynth. Res*. 56: 103–112.

Kromdijk, J., Głowacka, K., Leonelli, L., Gabilly, S.T., Iwai, M., Niyogi, K.K., et al. (2016) Improving photosynthesis and crop productivity by accelerating recovery from photoprotection. *Science* 354: 857–861.

Laisk, A., Kiirats, O., Eichelmann, H. and Oja, V. (1987) Gas exchange studies of carboxylation kinetics in intact leaves. *In* Progress in Photosynthesis Research. Edited by Biggins J. pp. 245–252. Springer, Dordrecht, Netherlands.

Laisk, A., Kiirats, O. and Oja, V. (1984) Assimilatory power (postillumination CO2 uptake) in leaves: measurement, environmental dependencies, and kinetic properties. *Plant Physiol.* 76: 723–729.

Laisk, A., Talts, E., Oja, V., Eichelmann, H. and Peterson, R.B. (2010) Fast cyclic electron transport around photosystem I in leaves under far-red light: a proton-uncoupled pathway? *Photosynth. Res.* 103: 79–95.

Li, X., Björkman, O., Shih, C., Grossman, A.R., Rosenquist, M., Jansson, S., et al. (2000) A pigment-binding protein essential for regulation of photosynthetic light harvesting. *Nature* 403: 391–395.

Miyake, C. (2010) Alternative electron flows (water-water cycle and cyclic electron flow around PSI) in photosynthesis: Molecular mechanisms and physiological functions. *Plant Cell Physiol*. 51: 1951–1963.

Miyake, C., Ulrich, S. and Kozi, A. (1995) Ferredoxin-dependent and antimycin a-sensitive reduction of cytochrome *b*-559 by far-red light in maize thylakoids; participation of a menadiol-reducible cytochrome *b*-559 in cyclic electron flow. *Plant Cell Physiol*. 36: 743–749.

Myers, J. (1971) Enhancement studies in photosynthesis. *Annu. Rev. Plant Physiol.* 22: 289–312.

Niyogi, K.K., Grossman, A.R. and Bjorkman, O. (1998) Arabidopsis mutants define a central role for the xanthophyll cycle in the regulation of photosynthetic energy conversion. *Plant Cell* 10: 1121.

Oxborough, K. and Baker, N.R. (1997) Resolving chlorophyll a fluorescence of photosynthetic efficiency into photochemical components—calculation of qP and Fv′/Fm′ without measuring Fo′. *Photosynth. Res*. 54: 135–142.

Pearcy, R.W. (1990) Sunflecks and photosynthesis in plant canopies. *Annu. Rev. Plant Physiol. Plant Mol. Biol.* 41: 421–453.

Pearcy, R.W., Krall, J.P. and Sassenrath-Cole, G.F. (1996) Photosynthesis in fluctuating light environments. *In* Photosynthesis and the Environment. Edited by Baker, N. R. pp. 321–346. Kluwer Academic Publishers, Dordrecht.

Pérez-Bueno, M.L., Johnson, M.P., Zia, A., Ruban, A.V. and Horton, P. (2008) The Lhcb protein and xanthophyll composition of the light harvesting antenna controls the ΔpH-dependency of non-photochemical quenching in *Arabidopsis thaliana*. *FEBS Lett*. 582: 1477–1482.

Pons, T.L. and Pearcy, R.W. (1992) Photosynthesis in flashing light in soybean leaves grown in different conditions. II. Lightfleck utilization efficiency. *Plant. Cell Environ.* 15: 577–684.

Roden, J.S. and Pearcy, R.W. (1993) Photosynthetic gas exchange response of poplars to steady-state and dynamic light environments. *Oecologia* 93: 208–214.

Ruban, A. (2013) *The Photosynthetic Membrane: molecular Mechanisms and Biophysics of Light Harvesting*. John Wiley & Sons, Ltd, Chichester, UK.

Ruban, A.V. (2016) Nonphotochemical chlorophyll fluorescence quenching: mechanism and effectiveness in protecting plants from photodamage. *Plant Physiol.* 170: 1903–1916.

Sacksteder, C.A., Kanazawa, A., Jacoby, M.E. and Kramer, D.M. (2000) The proton to electron stoichiometry of steady-state photosynthesis in living plants: a proton-pumping Q cycle is continuously engaged. *Proc. Natl. Acad. Sci. USA* 97: 14283–14288.

Sharkey, T.D., Seemann, J.R. and Pearcy, R.W. (1986) Contribution of metabolites of photosynthesis to postillumination CO2 assimilation in response to lightflects. *Plant Physiol.* 82: 1063–1068.

Smith, H. (1982) Light quality, photoperception, and plant strategy. *Annu. Rev. Plant Physiol.* 33: 481–518.

Sonoike, K. (1996) Degradation of psaB gene product, the reaction center subunit of photosystem I, is caused during photoinhibition of photosystem I: possible involvement of active oxygen species. *Plant Sci.* 115: 157–164.

Suorsa, M., Jarvi, S., Grieco, M., Nurmi, M., Pietrzykowska, M., Rantala, M., et al. (2012) PROTON GRADIENT REGULATION5 is essential for proper acclimation of Arabidopsis photosystem I to naturally and artificially fluctuating light conditions. *Plant Cell* 24: 2934–2948.

Takagi, D., Amako, K., Hashiguchi, M., Fukaki, H., Ishizaki, K., Goh, T., et al. (2017) Chloroplastic ATP synthase builds up a proton motive force preventing production of reactive oxygen species in photosystem I. *Plant J.* 91: 306–324.

Takagi, D., Takumi, S., Hashiguchi, M., Sejima, T. and Miyake, C. (2016) Superoxide and singlet oxygen produced within the thylakoid membranes both cause photosystem I photoinhibition. *Plant Physiol.* 171: 1626–1634.

Tasker, R. and Smith, H. (1977) the Function of phytochrome in the natural environment–V. Seasonal changes in radiant energy quality in woodlands. *Photochem. Photobiol.* 26: 487–491.

Way, D.A. and Pearcy, R.W. (2012) Sunflecks in trees and forests: from photosynthetic physiology to global change biology. *Tree Physiol.* 32: 1066–1081.

Wraight, C. A. and Crofts, A. R. (1970) Energy-dependent quenching of chlorophyll alpha fluorescence in isolated chloroplasts. *Eur. J. Biochem.* 17: 319–327.

Yamamoto, H.Y., Nakayama, T.O.M. and Chichester, C.O. (1962) Studies on the light and dark interconversions of leaf xanthophylls. *Arch. Biochem. Biophys.* 97: 168–173.

Yamori, W., Makino, A. and Shikanai, T. (2016) A physiological role of cyclic electron transport around photosystem I in sustaining photosynthesis under fluctuating light in rice. *Sci. Rep.* 6: 1–12.

Zhu, X.G., Ort, D.R., Whitmarsh, J. and Long, S.P. (2004) The slow reversibility of photosystem II thermal energy dissipation on transfer from high to low light may cause large losses in carbon gain by crop canopies: a theoretical analysis. *J. Exp. Bot.* 55: 1167–1175.